

- T. A. Stone, R. F. Nelson, W. Kovalick, *J. Geophys. Res.* **92**, 2157 (1987).
20. A. W. Setzer and M. C. Pereira, *Ambio* **20**, 19 (1991); A. W. Setzer, *Relatorio INPE-4534-RPE/565* (Instituto Nacional de Pesquisas Espaciais, São José dos Campos, Brazil, 1988).
21. *Anuário Estatístico do Brasil 1991* (Fundação Instituto Brasileiro de Geografia e Estatística, Rio de Janeiro, Brazil, 1991), vol. 51, pp. 1–1024.
22. *Mapa de Vegetação do Brasil* (Fundação Instituto Brasileiro de Geografia e Estatística, Rio de Janeiro, Brazil, 1988).
23. D. L. Skole, thesis, University of New Hampshire (1992).
24. Images: 7 from 1989, 175 from 1988, 8 from 1987, and 20 from 1986. All data from the Brazilian Landsat receiving station. The exact boundary between intact forest and deforested land was digitized in the Universal Transverse Mercator projection and then edited and error-checked with use of clear velum plots of the line-work overlaid on each photographic image. Each Landsat scene contained coordinate control points in decimal degree units, such that each scene could be geographically registered within precise tolerances and mosaicked together. For digitization, vertices were placed approximately every 50 m of ground position. Tests of positional accuracy in digitizing followed those of R. Dunn, R. Harrison, and J. C. White [*Int. J. Geograph. Inf. Syst.* **4**, 385 (1990)] and indicated encoding; hence, area-estimation errors were less than 3% (23). The variance associated with interpretation and delineation of boundaries between intact forest and deforested areas was less than 10% overall. Further accuracy assessment was made in test sites established in Rondonia, where fragmentation was very high. An explicit spatial comparison between our estimate of deforestation and the same derived from high-resolution (20-m resolution) SPOT satellite imagery was highly correlated ($r^2 = 0.98$; $y = 1.11x - 57.358$). Additional ground checking and verification was done in eastern Para state (north of Manaus) and along the Rio Negro, both in Amazonas.
25. Fundamental to our analysis was a specified representation for water, cerrado or savanna, and forest for the Brazilian Amazon. We used a vegetation map (23) that was augmented by Landsat Thematic Mapper and meteorological satellite imagery for more accurate depiction of cerrado and water. This GIS representation is available upon request.
26. R. B. Buschbacher, *BioScience* **36**, 22 (1986); C. Uhl, R. B. Buschbacher, E. A. S. Serrao, *J. Ecol.* **76**, 663 (1988); R. B. Buschbacher, C. Uhl, E. A. S. Serrao, *ibid.*, p. 682.
27. This work was supported by National Aeronautics and Space Administration's mission to planet Earth and the Eos Data Information System's Landsat Pathfinder Program. We acknowledge S. Tilford and W. Huntress for initiating this research, W. Chomentowski for assistance in developing the satellite and GIS database, and A. Nobre for his assistance in interpreting the satellite data. G. Batista, M. Heinicke, and T. Grant assisted with the GIS representation of forest, water, and cerrado.

RESEARCH ARTICLE

Arrestin Function in Inactivation of G Protein–Coupled Receptor Rhodopsin in Vivo

Patrick J. Dolph, Rama Ranganathan, Nansi J. Colley, Robert W. Hardy, Michael Socolich, Charles S. Zuker*

Arrestins have been implicated in the regulation of many G protein–coupled receptor signaling cascades. Mutations in two *Drosophila* photoreceptor-specific arrestin genes, *arrestin 1* and *arrestin 2*, were generated. Analysis of the light response in these mutants shows that the Arr1 and Arr2 proteins are mediators of rhodopsin inactivation and are essential for the termination of the phototransduction cascade in vivo. The saturation of arrestin function by an excess of activated rhodopsin is responsible for a continuously activated state of the photoreceptors known as the prolonged depolarized afterpotential. In the absence of arrestins, photoreceptors undergo light-dependent retinal degeneration as a result of the continued activity of the phototransduction cascade. These results demonstrate the fundamental requirement for members of the arrestin protein family in the regulation of G protein–coupled receptors and signaling cascades in vivo.

Rhodopsin is a member of a class of receptors containing seven membrane-spanning domains that transduce extracellular signals to specific intracellular effector molecules through the activation of heterotrimeric guanosine triphosphate–binding proteins (G proteins). This large superfamily of proteins, collectively known as G protein–coupled receptors, includes receptors for a variety of environmental signals such as hormones, neurotransmitters, peptides, light, and odorants (1, 2).

The events that lead to the stimulation of

G protein–coupled receptors, and the subsequent activation of their corresponding effector molecules [such as adenylyl cyclase, guanosine 3',5'-monophosphate (cGMP) phosphodiesterase, and phospholipase C] have been well characterized (2, 3). However, the mechanisms effecting the termination of the activated state of these receptors and the downstream signaling molecules in vivo are not well defined. Such information is essential for an understanding of the regulation of receptor function and the role of this regulation in modulating receptor-mediated cellular processes.

Much of the data on mechanisms of inactivation of G protein–coupled receptors has come from in vitro reconstitution studies of the β -adrenergic receptor (4, 5) and

bovine rhodopsin (6). The inactivation of metarhodopsin, the activated state of rhodopsin, is thought to result from the action of at least two proteins, rhodopsin kinase and arrestin. According to this model, light-activated rhodopsin is a substrate for rhodopsin kinase, which phosphorylates rhodopsin in a cluster of serine-threonine residues located in the COOH-terminal tail of the protein (7–9). The light-activated, phosphorylated rhodopsin interacts stoichiometrically with arrestin, an abundant cytosolic protein that competes with the G protein for receptor binding and terminates, or arrests, the activated state of the receptor (10, 11). Although this model is consistent with biochemical studies of arrestin function in vitro, little is known about the function of this protein in vivo (12).

Arrestin was originally identified as an abundant, soluble 48-kD protein (also known as soluble antigen or S antigen) found in the vertebrate retinal and pineal photoreceptors (13). Human and bovine S antigen are highly immunogenic and have been linked to autoimmune disorders that affect vision (14). Functional homologs of visual arrestin have been isolated from non-retinal tissue and have been implicated in the desensitization and inactivation of the β -adrenergic receptor (β arrestins) (15–17). Similar proteins have been thought to act as mediators of the inactivation of many G protein–coupled receptors (18) and therefore, the molecular mechanisms of receptor inactivation may be shared among members of this receptor superfamily.

Drosophila provides an excellent model system for studying the function of arrestin and the regulation of G protein–coupled receptors in vivo (19–21). Mutants with defects in key regulatory components of the phototransduction cascade can be isolated and studied genetically, physiologically, and biochemically. Phototransduction in *Drosophila* begins with the light activation of rhodopsin (19, 21). Rhodopsin consists

The authors are in the Howard Hughes Medical Institute and Departments of Biology and Neurosciences, University of California at San Diego, La Jolla, CA 92093–0049.

*To whom correspondence should be addressed.

of the apoprotein opsin, covalently linked to a chromophore, generally 11-*cis*-retinal. Absorption of a photon causes the isomerization of the chromophore from the 11-*cis* to the all-*trans* configuration, and results in a conformational shift in rhodopsin and the activation of its catalytic properties. Activated rhodopsin interacts with a visual system-specific G protein (22) that activates a phospholipase C (PLC). The PLC hydrolyzes the membrane phospholipid phosphatidylinositol-4,5-bisphosphate (PIP₂) into the two intracellular messengers inositol triphosphate (IP₃) and diacylglycerol (DAG). The IP₃ mobilizes calcium from intracellular stores and leads to the eventual opening of cation-selective ion channels which results in the generation of a receptor potential (23). Termination of the receptor potential requires the inactivation of all of the excitatory intermediates involved in the phototransduction cascade, including metarhodopsin.

Genes encoding two visual system-specific arrestins, *arrestin 1* (*arr1*) and *arrestin 2* (*arr2*), have been isolated in *Drosophila* (24–27). The Arr1 protein is a 37-kD polypeptide and shares 51 percent amino acid identity with the Arr2 protein (48 kD) and 43 percent identity with the vertebrate visual arrestin molecule. To study the function of arrestins in the modulation of G protein-coupled receptor activity *in vivo*, we used a combined genetic, physiological, and cell biological approach to study *Drosophila* mutants with defects in arrestin function.

Isolation and characterization of arrestin mutants. To gain insight into the function of arrestins *in vivo*, we used a genetic screen to isolate mutations in the *Drosophila* arrestin genes. Several obstacles in setting up a screen to isolate mutations in the arrestin genes were the lack of a predictable phenotype that defines their loss of function and the possibility that *arr1* and *arr2* may serve redundant functions. We therefore used a screening strategy that was based on the loss of arrestin antigens on immunoblots (28) instead of on a hypothetical physiological or behavioral defect.

To determine more precisely the cellular distribution of each of the *Drosophila* arrestins we generated transgenic animals that express a chimeric gene consisting of the promoter of *arr1* or *arr2* fused to a *lacZ* reporter gene with a nuclear localization signal and examined the expression of *lacZ*. Both arrestin-reporter transgenes are expressed in all of the photoreceptors of the adult visual system (Fig. 1, A and B). We also examined the subcellular distribution of Arr1 and Arr2 proteins by immunocytochemical analysis of frozen tissue sections of adult heads. The results show that the

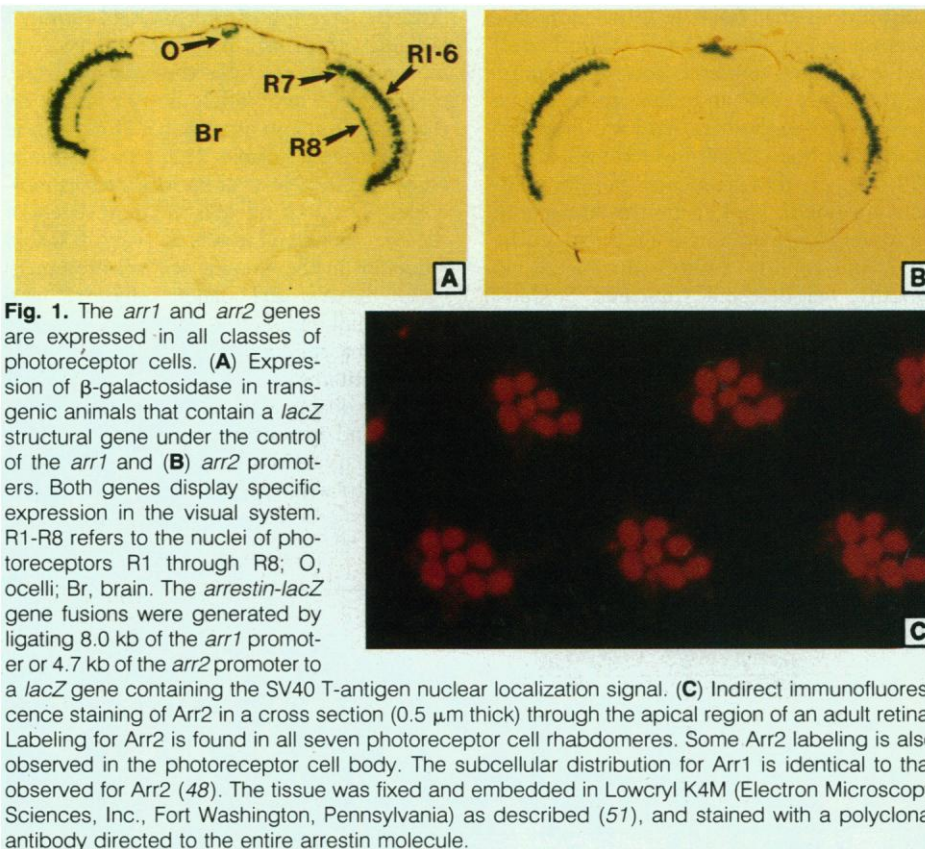


Fig. 1. The *arr1* and *arr2* genes are expressed in all classes of photoreceptor cells. (A) Expression of β -galactosidase in transgenic animals that contain a *lacZ* structural gene under the control of the *arr1* and (B) *arr2* promoters. Both genes display specific expression in the visual system. R1-R8 refers to the nuclei of photoreceptors R1 through R8; O, ocelli; Br, brain. The *arrestin-lacZ* gene fusions were generated by ligating 8.0 kb of the *arr1* promoter or 4.7 kb of the *arr2* promoter to a *lacZ* gene containing the SV40 T-antigen nuclear localization signal. (C) Indirect immunofluorescence staining of Arr2 in a cross section (0.5 μ m thick) through the apical region of an adult retina. Labeling for Arr2 is found in all seven photoreceptor cell rhabdomeres. Some Arr2 labeling is also observed in the photoreceptor cell body. The subcellular distribution for Arr1 is identical to that observed for Arr2 (48). The tissue was fixed and embedded in Lowcryl K4M (Electron Microscopy Sciences, Inc., Fort Washington, Pennsylvania) as described (51), and stained with a polyclonal antibody directed to the entire arrestin molecule.

arrestin proteins are primarily localized in the rhabdomeres (Fig. 1C), which are the specialized microvillar organelles containing the visual pigment rhodopsin and most of the phototransduction proteins (19). The localization of Arr1 and Arr2 to the rhabdomeres is consistent with a role for these proteins in the phototransduction cascade. The colocalization of both arrestins to all of the photoreceptor cells raised the possibility that *arr1* and *arr2* may serve redundant functions and that mutations in only one gene may lack a phenotype. Therefore, we screened for mutations in each arrestin gene.

To carry out the immunoblot screen for mutations in *arr1* and *arr2*, we generated antibodies to peptides specific to the COOH-terminus of each protein (Fig. 2). Such antibodies would not recognize the truncated proteins produced as a result of nonsense mutations located upstream in the open reading frame from the COOH-terminus used to generate the antibodies, and would therefore be scored as protein nulls. Because Arr2 is the most abundant arrestin in the *Drosophila* retina, we focused on generating mutants at this locus first. The *arr2* gene is located on the third chromosome at position 66D^{10–11}. Figure 2 shows the structure of the gene and adjacent chromosomal DNA, and presents a diagram describing the genetic scheme used in our mutagenesis screen. Single fly

heads were removed from animals that were homozygous for mutagenized third chromosomes and were screened for the loss of Arr2 immunoreactivity by protein immunoblot analysis (Fig. 3). To control for the amount of material in each lane, we simultaneously probed with an antibody to Arr1. Because *arr1* maps to the second chromosome, which was not homozygosed in this screen, no mutations in *arr1* were expected to be detected. We screened 11,429 mutagenized chromosomes and recovered a single *arr2* allele, *arr2*¹. Using the *arr2*¹ allele, we designed a more efficient genetic screen to search for additional alleles (29). We then screened an additional 9,371 chromosomes and isolated two more *arr2* alleles, *arr2*² and *arr2*³.

To isolate mutations in *arr1*, we made use of a large chromosomal deficiency that deletes the *arr1* gene (Fig. 2C). Single heads from flies heterozygous for this chromosomal deficiency and mutagenized chromosomes were screened for the loss of the Arr1 antigen on immunoblots as described. We screened 15,481 mutagenized chromosomes and recovered two *arr1* alleles, *arr1*¹ and *arr1*².

Using the polymerase chain reaction, we isolated the *arr1* and *arr2* genes from each of the arrestin mutants and determined their entire nucleotide sequence (30). All three *arr2* alleles contain single nucleotide

substitutions that result in either nonsense or missense mutations (Table 1). Both *arr2*¹ and *arr2*² have nonsense codons at amino acid residues 356 and 363, respectively. Because the antibody to Arr2 was produced from a peptide containing residues 370 to 379 (Fig. 2), these truncated protein products are not recognized by this antiserum. However, using an antiserum to the entire Arr2 polypeptide (401 amino acids in length), we detected truncated products that differed from the wild-type protein by the predicted size (31). The *arr2*¹ and *arr2*² alleles produce truncated proteins expressed at approximately 80 and 20 percent of the amount of wild-type Arr2 protein, respectively. Because the primary structure of Arr1 (364 amino acid residues) differs from

Arr2 by having a shorter COOH-terminal tail (26), these *arr2* mutants produce Arr2 molecules that resemble the wild-type Arr1 protein. The *arr2*³ allele has an alteration that substitutes an aspartic acid for a valine at residue 52 (Table 1). This valine is conserved in nearly all known arrestin molecules. The *arr2*³ allele is the most severe of the *arr2* alleles and results in over a 100-fold reduction in the amount of Arr2 protein.

Of the two *arr1* alleles, only *arr1*² is a protein null mutation; it contains a missense mutation at residue 154 (Table 1). The *arr1*¹ allele contains a 5-kb insertion of foreign DNA (probably a transposable element) in the second intron and produces a mutant protein expressed at approximately 10 percent of the wild-type levels of Arr1 protein.

The *arr2* mutants are defective in photoreceptor cell deactivation. Using whole cell patch-clamp recordings, we have analyzed the electrophysiological responses of *arr2* mutant photoreceptors to light stimuli. The responses of wild-type and mutant photoreceptors to 10-ms flashes of light are shown (Fig. 4). The kinetics of the light response in wild-type cells display rapid deactivation (defined as the recovery of the photoresponse after termination of the stimulus) (Fig. 4A). In contrast, *arr2*³ mutant photoreceptors exhibit a large decrease in the rate of deactivation (Fig. 4, B and G). For quantitative evaluation of the data, the tail of the deactivation phase of the light-activated current was fitted to a single exponential function and the time constant

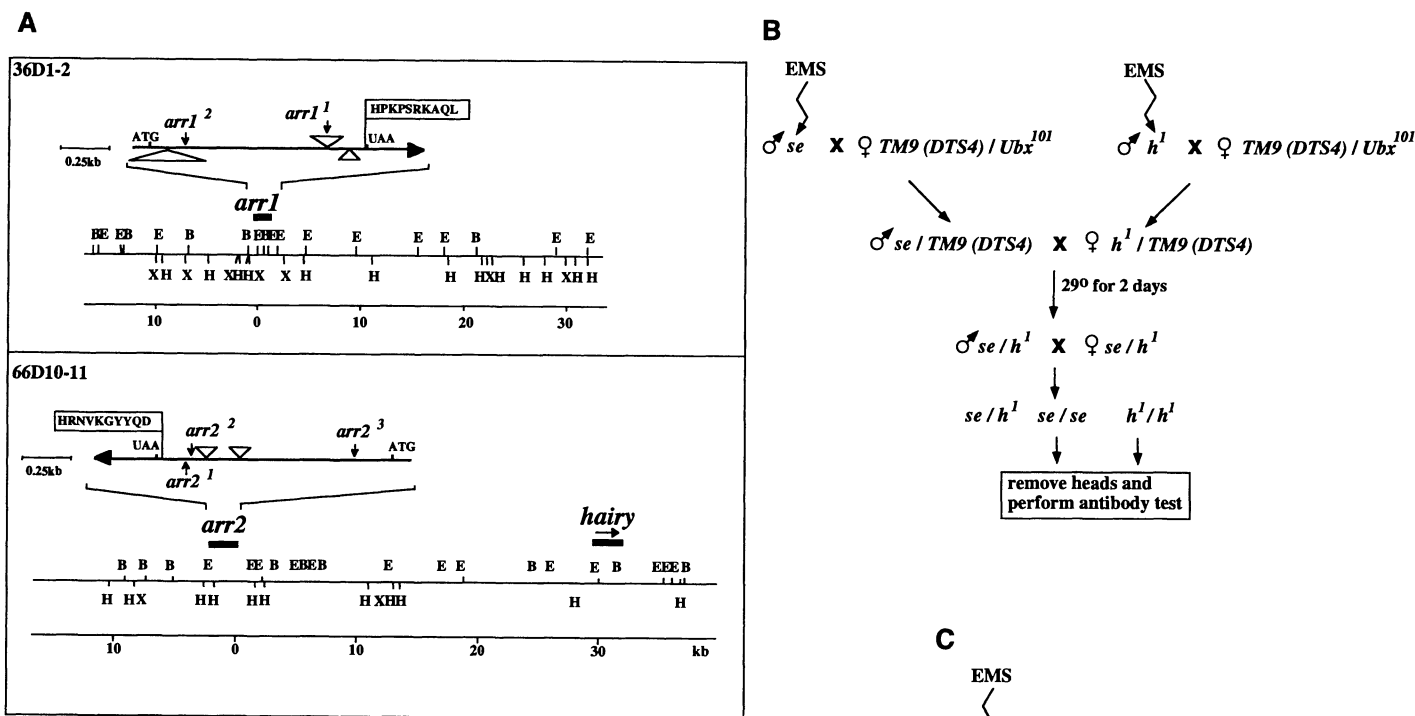


Fig. 2. (A) Genomic walk of the 36D and 66D chromosomal regions that contain the arrestin genes. A chromosomal walk was initiated from the *arr1*, *arr2*, and *hairy* (*h*) genes. Overlapping clones were isolated from a lambda FIX II genomic library. The expanded diagram above the map shows the detailed structure of each arrestin gene. Small triangles indicate introns and arrows point to the location of mutations isolated in this study. Horizontal arrows denote the direction of transcription of the *arr1*, *arr2*, and *h* genes. The flag above each gene displays the location and sequence of the peptide used to produce the isoform-specific antisera. Restriction endonuclease sites are B, Bam HI; E, Eco RI; H, Hind III; X, Xho I. (B) Genetic screen used for isolation of *arr2* mutants. There are no chromosomal deficiencies available for this region and repeated attempts to generate deficiencies were unsuccessful, presumably due to the presence of a haplo-lethal gene nearby. Chromosomes marked with *hairy* and *sepia* (*se*) were used because of their close genetic linkage with the *arr2* locus. Males of each genotype were aged for 2 days, treated with EMS (52), and crossed as a group to females carrying the *dominant temperature sensitive 4* (*DTS4*) marker in a *TM9* balancer. Mutagenizing two differently marked stocks permitted screening twice as many chromosomes per cross. The F1 males and F1 virgin females were collected and crossed in single male-female matings. The flies were allowed to lay eggs for 48 hours and then shifted to 29°C to eliminate any eggs or larvae carrying the *DTS4* allele. The parents were then removed and the vials

were incubated at 29°C for an additional 48 hours before they were returned to 25°C. The progeny from this cross were transferred to fresh food and cleared after 5 days, and their homozygous *sepia* or *hairy* progeny were subjected to the protein immunoblot screen for the loss of the Arr2 antigen. (C) Screen used to generate mutations in the *arr1* locus. EMS-treated *cinnabar brown* (*cn bw*) males were crossed to flies carrying a deficiency that uncovers the *arr1* locus (53). Single F1 males were backcrossed to the deficiency bearing strain, and the non-*Curly* (*Cy*) progeny were subjected to protein immunoblot analysis.

(τ) was measured (32). This analysis showed that wild-type photoreceptors have deactivation time constants of 18.8 ± 2.9 ms, whereas *arr2* mutants have time constants of 166.9 ± 28.1 ms. To demonstrate that this phenotype is due solely to the loss

of Arr2 protein, we carried out P element-mediated germ-line transformation of the cloned *arr2*⁺ gene into *arr2* mutant hosts. The reintroduction of a wild-type copy of the *arr2* gene fully rescues the defects in *arr2* mutants and restores wild-type visual physi-

ology (Fig. 4, C and G). Together, these results demonstrate that Arr2 is a key mediator of photoreceptor cell deactivation.

The *arr2*¹ and *arr2*² alleles produce truncated polypeptides in which the last 46 and 39 residues have been deleted (Table 1). Bovine arrestin truncated in the homologous COOH-terminal region (last 40 to 60 residues) binds in vitro not only to photoactivated, phosphorylated rhodopsin but also to phosphorylated rhodopsin that has not been light activated (33, 34). On the basis of these observations, it was suggested that the COOH-terminus of arrestin is required to confer substrate specificity (33, 34). To determine whether such truncations have an effect in vivo on the phototransduction process, we studied the visual physiology of *arr2*¹ mutants. The records of the light-activated responses of *arr2*¹ photoreceptors (Fig. 4D) show wild-type kinetics, suggesting that this region of arrestin is not required for normal function in vivo. Our additional studies of the physiology of these arrestin truncation mutants have not uncovered a visual defect (35).

The *arr2* mutants are specifically defective in the inactivation of metarhodopsin. In wild-type photoreceptors, inactivation of the biologically active state of rhodopsin (metarhodopsin) is not the rate-limiting step in the deactivation of the light response (36). Rather, termination of the light response results from the orchestrated action of feedback regulatory mechanisms at the level of receptor, G protein, effector molecule, and ion channels.

In physiologically normal photoreceptors, deactivation of the light response becomes faster as the light intensity of the stimulus is increased (Fig. 5A). This is a property of both vertebrate and invertebrate photoreceptors, and results from the activation of adaptation mechanisms (37). In contrast, *arr2* mutant photoreceptors show deactivation kinetics in which higher light intensities cause even slower deactivation rates (Fig. 5B). Thus, the termination of the light-activated currents in *arr2* mutants may be rate-limited by a different

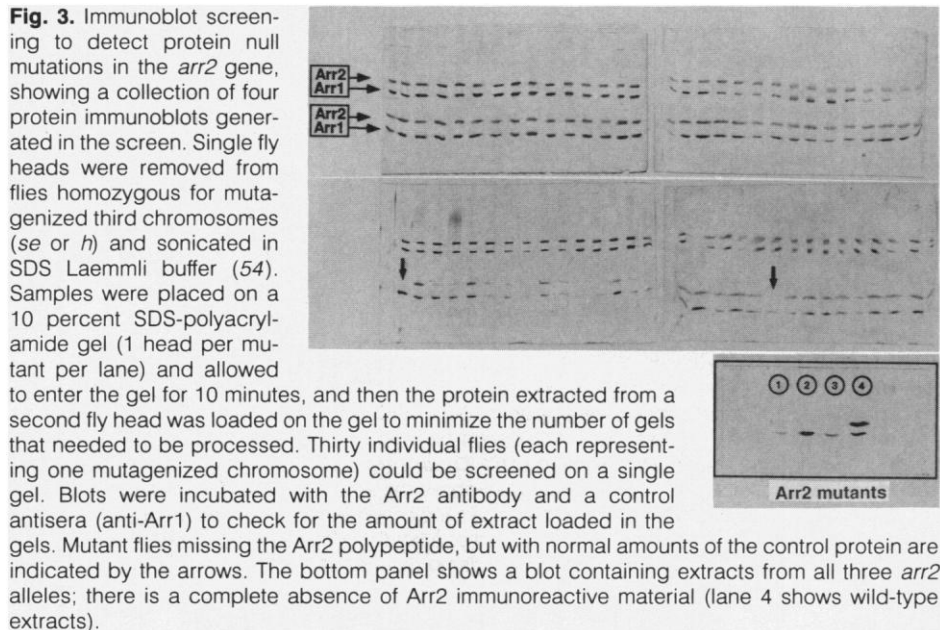


Fig. 3. Immunoblot screening to detect protein null mutations in the *arr2* gene, showing a collection of four protein immunoblots generated in the screen. Single fly heads were removed from flies homozygous for mutagenized third chromosomes (*se* or *h*) and sonicated in SDS Laemmli buffer (54). Samples were placed on a 10 percent SDS-polyacrylamide gel (1 head per mutant per lane) and allowed to enter the gel for 10 minutes, and then the protein extracted from a second fly head was loaded on the gel to minimize the number of gels that needed to be processed. Thirty individual flies (each representing one mutagenized chromosome) could be screened on a single gel. Blots were incubated with the Arr2 antibody and a control antisera (anti-Arr1) to check for the amount of extract loaded in the gels. Mutant flies missing the Arr2 polypeptide, but with normal amounts of the control protein are indicated by the arrows. The bottom panel shows a blot containing extracts from all three *arr2* alleles; there is a complete absence of Arr2 immunoreactive material (lane 4 shows wild-type extracts).

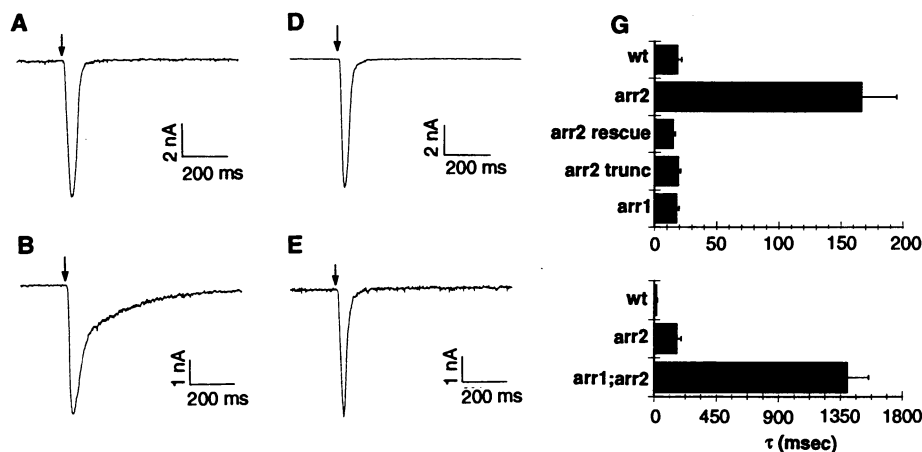


Fig. 4. Defects shown by arrestin mutants in photoreceptor deactivation. Whole-cell voltage clamp recordings of light-activated currents from (A) wild-type, (B) *arr2*³, (C) *arr2*³; *P*[*w*⁺, *arr2*] transgenic animals, (D) *arr2*¹, (E) *arr1*², and (F)

*arr1*¹; *arr2*³ double mutants. Responses are to 10-ms flashes of light at holding potentials of -40 mV. Preparations of isolated *Drosophila* photoreceptors and patch-clamp methods were as described (55). Recordings were made in symmetric Cs⁺ solutions with $500 \mu\text{M}$ Ca²⁺ in the bath [the pipette solution consisted of 124 mM CsCl, 10 mM Hepes, 0.1 mM EGTA, 10 μM CaCl₂, 2 mM MgCl₂, 3 mM Mg²⁺-ATP, and 0.5 mM Na⁺-GTP (pH 7.15); the bath solution consisted of 124 mM CsCl, 10 mM Hepes, 500 μM CaCl₂, and 32 mM sucrose (pH 7.15)]. Photoreceptors were stimulated with monochromatic light at $\lambda = 480 \pm 10$ nm. (G) For quantitation of photoreceptor deactivation, tail currents of the light response were fitted to a single exponential function (32). A minimum of four different cells, representing at least ten individual electrophysiological recordings, were characterized in each case. Time constants (\pm SD) were: wt = 18.8 ± 2.9 , *arr2*³ = 166.9 ± 28.1 , *arr2*³ rescue = 15.2 ± 1.5 , *arr1*² = 18.1 ± 1.5 , *arr2*¹ = 19.5 ± 1.4 , and *arr1*; *arr2* = 1402.5 ± 150.9 .

Table 1. Molecular characterization of mutations in the *arr1* and *arr2* genes, and the quantification of protein from the mutant alleles (30) relative to wild-type.

Allele	Changes		Protein (%) [†]
	Nucleotide [*]	Amino acid	
<i>arr1</i> ¹	DNA insertion \ddagger		~10
<i>arr1</i> ²	T ¹⁰⁰¹ → A	C ¹⁵⁴ → S	<1
<i>arr2</i> ¹	A ¹²⁷³ → T	K ³⁵⁶ → STOP	~80
<i>arr2</i> ²	A ¹²⁹⁴ → T	K ³⁶³ → STOP	~10 to 20
<i>arr2</i> ³	T ³⁶² → A	V ⁵² → D	<1

^{*}Numbered according to (25 and 26). [†]Percent of wild-type. [‡]As described in the text.

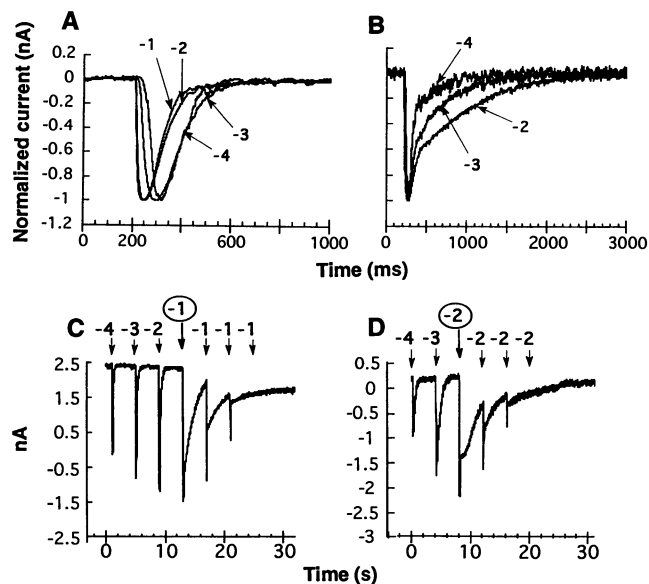
process from that in wild-type. Because the deactivation rate of the photoreceptor cell response in *arr2* mutants is inversely dependent on the amount of activated rhodopsins (that is, a function of light intensity), it is possible that inactivation of metarhodopsin has become the rate-limiting step in the termination of the light response.

Direct evidence for defects in metarhodopsin inactivation in *arr2* mutants is provided by the analysis of the prolonged depolarizing afterpotential (PDA). A PDA is a sustained photoreponse that occurs in wild-type photoreceptors whenever a substantial amount of rhodopsin has been photoconverted from R to the active M state (Fig. 5C) (39). During a PDA, photoreceptors are refractory to light stimuli, and thus cannot respond to further visual input. Unlike vertebrate opsins, most invertebrate photopigments are not bleached after light activation but can instead be photoconverted between the rhodopsin form (R form) and a thermally stable biologically active metarhodopsin (M) form (38). The major rhodopsin in the fly retina has an R form with an absorption maximum at 480 nm and an M form with an absorption maximum at 580 nm. The wide spectral separation between these two forms permits effective and reproducible experimental manipulation of the two states of the light receptor molecule. A PDA can be terminated at any time by photoconversion of metarhodopsin back to rhodopsin. This suggests that the continued activity of metarhodopsin sustains the afterpotential, and that a PDA is the result of the loss of the normal metarhodopsin inactivation process.

Because arrestin may be involved in the inactivation of metarhodopsin, we examined whether defects in arrestin function could lead to defects in the PDA process. Wild-type photoreceptors require approximately 20 percent conversion of R to M to trigger a PDA (38). This amount of rhodopsin isomerization is approximately equal to the total number of arrestin molecules in the photoreceptor cell (26, 40). If arrestin and rhodopsin interact stoichiometrically, then the saturation of free arrestin may be the basis for the PDA. Consistent with this hypothesis, *arr2* mutants undergo a PDA with 10 times less photoconversion of R to M than is observed in wild-type (Fig. 5D). These results indicate that a PDA may represent not only the presence of excess metarhodopsin over free arrestin, but also that arrestin is required for the normal mechanisms of metarhodopsin inactivation.

Because a PDA requires a substantial net shift in the absolute amount of rhodopsin to the metarhodopsin form, mutants with reduced concentrations of rhodopsin do not

Fig. 5. The kinetics of photoreceptor cell deactivation in *arr2* mutants is dependent on the fraction of activated rhodopsin molecules. (A) Deactivation kinetics of wild-type and (B) *arr2*³ photoreceptors as a function of light intensity. Each graph shows four traces of light-activated currents recorded from the same photoreceptor cell at increasing light intensities. Arrows are labeled with the relative log order of light intensity [$\log(I/I_0)$], where I_0 is the maximum intensity produced by the stimulating light source (0.812 mW/cm²). Therefore, for example, -4 represents 10 times less light than -3, and this value is 10 times less light than -2. Photoreceptors were given a 10-ms light flash at a holding potential of -40 mV. Traces are normalized to peak current. Different time scales are used in wild-type and *arr2*³ mutants. (C) Induction of a PDA in wild-type and (D) *arr2*³ mutants. Arrows indicate the position of 480-nm light flashes of 10-ms duration. Numbers above the arrows indicate the relative log order of light intensity (as described in A). Circled numbers indicate the minimum amount of light required to trigger a PDA. Light responses were recorded at a holding potential of -40 mV. Recordings in (A) to (D) are representative whole-cell voltage-clamp recordings.



undergo a PDA (Fig. 6B). Pak and co-workers have isolated a collection of *Drosophila* mutants [*nina* (*neither-inactivation-nor-afterpotential*) mutants] that cannot be induced to trigger and support a PDA (41). Each of the eight *nina* complementation groups encodes a gene involved in rhodopsin synthesis (42), structure (43), or metabolism (44), or genes that affect rhabdomere structure (45) such that less rhodopsin is present in the photoreceptor cells. In our model, it should be possible to generate a PDA in such mutants provided that there is a corresponding reduction in the level of arrestins. To test our model, we generated flies that are double mutants for two different *ninaA* alleles and *arr2*³. The *ninaA*^{G89D} allele and the *ninaA*^{delT,F} allele produce 6 percent and 2 percent of the wild-type amounts of rhodopsin, respectively (46). Whereas the *ninaA* mutants themselves do not undergo a PDA, strong PDAs can be



Fig. 6. A prolonged depolarized afterpotential (PDA) is the result of excess metarhodopsin over available arrestin. Shown are electroretinogram recordings of (A) wild-type flies, (B) mutants with reduced rhodopsin levels (*ninaA*), and (C) mutants with reduced levels of rhodopsin and arrestin (*ninaA*; *arr2*³ double mutants). Shown are responses to maximum intensity 1-s flashes of 480-nm (R → M conversion) or 580-nm light (M → R conversion). Identical results were obtained with two different *ninaA* alleles, *ninaA*^{G89D} and *ninaA*^{delT,F}. Recordings were performed on white-eyed flies, stimulated with maximum light intensities as previously described (56).

triggered and supported (Fig. 6) in the double mutants. These results demonstrate that a PDA is the result of producing metarhodopsin in excess of free arrestin, and that the *nina* phenotype results from an excess of arrestin over rhodopsin.

Deactivation defects of *arr1* mutations are revealed in an *arr2* mutant background. Unlike the response in *arr2* mutants, the rate of photoreceptor cell deactivation in *arr1* mutants is similar to that in wild-type controls (Fig. 4, E and G). Because Arr2 is approximately five to seven times more abundant than Arr1 (26, 40), a loss of Arr2 protein represents the loss of a significant fraction of total arrestin in the cell. In contrast, loss of Arr1 protein represents only the loss of a small fraction of the total arrestin and thus may be expected to have only a slight effect on the kinetics of metarhodopsin inactivation.

To test if the lack of a phenotype in *arr1*

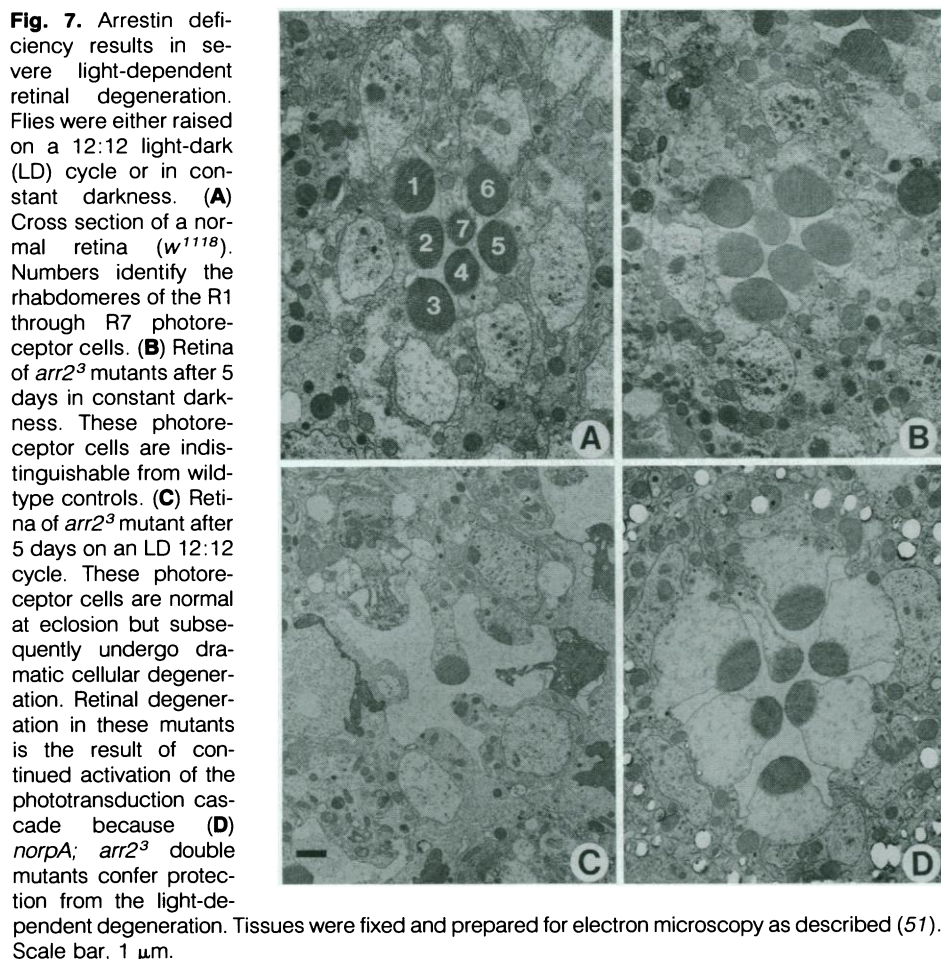


Fig. 7. Arrestin deficiency results in severe light-dependent retinal degeneration. Flies were either raised on a 12:12 light-dark (LD) cycle or in constant darkness. **(A)** Cross section of a normal retina (w^{1118}). Numbers identify the rhabdomeres of the R1 through R7 photoreceptor cells. **(B)** Retina of $arr2^3$ mutants after 5 days in constant darkness. These photoreceptor cells are indistinguishable from wild-type controls. **(C)** Retina of $arr2^3$ mutant after 5 days on an LD 12:12 cycle. These photoreceptor cells are normal at eclosion but subsequently undergo dramatic cellular degeneration. Retinal degeneration in these mutants is the result of continued activation of the phototransduction cascade because **(D)** $norpA$; $arr2^3$ double mutants confer protection from the light-dependent degeneration. Tissues were fixed and prepared for electron microscopy as described (51). Scale bar, 1 μ m.

mutants is the result of functional redundancy between Arr1 and Arr2, we constructed double mutants lacking both Arr1 and Arr2 proteins. Indeed, these double mutants have much slower deactivation kinetics than the $arr2^3$ mutant alone (Fig. 4F). For the double mutants, the increase in the deactivation time constant is more than 70 times that of a wild-type photoreceptor (Fig. 4G). Analysis of the PDA in the $arr1$; $arr2$ double mutants showed that less than one percent of the amount of light required to trigger a PDA in wild-type is sufficient to induce these photoreceptors into a prolonged depolarized state (35). This PDA reflects the activation of less than 0.2 percent of the rhodopsin molecules in these cells. Thus, unless the double mutants flies are raised in the dark, their photoreceptors readily enter a PDA state and are functionally inoperable. Together, these results demonstrate three important aspects of arrestin function in *Drosophila*. (i) Arr1 and Arr2 have a similar function in regulating photoreceptor cell deactivation. (ii) The deactivation of the visual response in $arr2$ mutants is primarily determined by Arr1. (iii) Although the termination of the phototransduction cascade in wild-type photoreceptors is determined by the con-

certed action of several feedback regulatory steps (20, 47), in the absence of arrestins the termination of the phototransduction process becomes rate-limited by the slow decay of metarhodopsin.

Mutations in the arrestin genes lead to light-dependent retinal degeneration. The finding that $arr2$ and $arr2$; $arr1$ double mutants enter a prolonged depolarized afterpotential with little light stimulation suggests that these animals may display pathological retinal defects as a result of the continuous activity of their photoreceptor cells. We tested this hypothesis by directly examining photoreceptor cell ultrastructure by transmission electron microscopy. The photoreceptors from $arr2^3$ flies display dramatic cellular degeneration 5 days after exposure to a 12 hour light–12 hour dark growth cycle (Fig. 7C). This degeneration is specifically the result of the loss of Arr2 function because transgenic $arr2^3$ flies expressing a wild-type copy of the $arr2$ gene have morphologically normal photoreceptor cells (48).

As predicted, $arr2^3$ mutants raised in the dark are morphologically indistinguishable from wild-type controls (Fig. 7, A and B). To demonstrate that the light-dependent retinal degeneration of arrestin mutants

results from the continued response of their activated photoreceptors, we generated flies mutant for both $arr2$ and the structural gene for the effector molecule of this signaling cascade, a phospholipase C encoded by the $norpA$ (*no receptor potential A*) locus (49). The $norpA$ mutation protects $arr2$ flies from retinal degeneration, demonstrating that the events responsible for degeneration occur downstream of PLC activation (Fig. 7D). Thus, the retinal degeneration observed in the arrestin mutants results from the continued activation of the phototransduction cascade. These results suggest that arrestin mutations in vertebrates are likely to lead to retinal dysfunction and may be part of the large group of human retinal degenerative disorders.

We have used a direct screening approach for the isolation of *Drosophila* mutants lacking arrestin function and have demonstrated that arrestin is essential for mediating metarhodopsin inactivation in vivo. The existence of arrestin homologs in G protein-coupled signaling cascades that utilize different effector molecules (2, 8, 23) suggests that the mechanisms of receptor inactivation are likely to be conserved (9, 10, 15, 17, 33, 50), and that these results may be generally applicable to members of this receptor superfamily.

The availability of arrestin mutants in *Drosophila* provides a genetic background suitable for structure-function studies of arrestin, and should permit to genetically identify and dissect arrestin regulatory pathways.

REFERENCES AND NOTES

1. J. Bockaert, *Current Opin. Neurobiol.* **1**, 32 (1991).
2. H. Dohlman, J. Thorner, M. Caron, R. Lefkowitz, *Annu. Rev. Biochem.* **60**, 653 (1991).
3. L. Stryer, *J. Biol. Chem.* **266**, 10711 (1991).
4. N. S. Roth, R. J. Lefkowitz, M. G. Caron, *Adv. Exp. Med. Biol.* **308**, 223 (1991).
5. S. Collins *et al.*, *Biochem. Soc. Trans.* **18**, 541 (1990).
6. K. Palczewski and J. Benovic, *Trends Biochem. Sci.* **16**, 387 (1991).
7. H. Kühn and W. J. Dreyer, *FEBS Lett.* **20**, 1 (1972).
8. H. Kühn, *Prog. Retinal Res.* **3**, 124 (1984).
9. K. Palczewski, J. H. McDowell, S. Jakes, T. S. Ingebritsen, P. A. Hargrave, *J. Biol. Chem.* **264**, 15770 (1989).
10. U. Wilden, S. Hall, H. Kühn, *Proc. Natl. Acad. Sci. U.S.A.* **83**, 1174 (1986).
11. H. Kühn and U. Wilden, *J. Receptor Res.* **7**, 298 (1987).
12. K. Palczewski, G. Rispoli, P. Detwiler, *Neuron* **8**, 117 (1992).
13. W. B. Wacker, L. A. Donoso, C. M. Kalsow, J. A. Yankeelov, D. T. Organisciak, *J. Immunol.* **119**, 1949 (1977); C. M. Kalsow and W. B. Wacker, *Invest. Ophthalmol. Visual Sci.* **16**, 181 (1977).
14. R. B. Nussenblatt, I. Gery, E. J. Ballintine, W. B. Wacker, *Am. J. Ophthalmol.* **89**, 173 (1980); R. B. Nussenblatt, T. Kuwabara, F. M. de Montasterio, W. B. Wacker, *Arch. Ophthalmol.* **99**, 1090 (1981).
15. M. J. Lohse, J. L. Benovic, J. Condina, M. G. Caron, R. J. Lefkowitz, *Science* **248**, 1547 (1990).
16. H. Attramada *et al.*, *J. Biol. Chem.* **267**, 17882 (1992).

17. M. J. Lohse *et al.*, *ibid.* p. 8558.
18. B. Rapoport, K. D. Kaufman, G. D. Chazenbalk, *Mol. Cell. Endocrinol.* **84**, R39 (1992); M. Mirshahi, A. Razaghi, S. S. Mirshahi, V. Van Tuyen, J. P. Faure, *Thromb. Res.* **64**, 551 (1991); U. Scheuring *et al.*, *FEBS Lett.* **276**, 192 (1990).
19. D. P. Smith, M. A. Stammes, C. S. Zuker, *Annu. Rev. Cell Biol.* **7**, 161 (1991).
20. R. Ranganathan, W. Harris, C. S. Zuker, *Trends Neurosci.* **14**, 486 (1991).
21. B. Minke and Z. Selinger, in *Prog. Retinal Res.* **11**, 99 (1992).
22. Y.-J. Lee, M. B. Dobbs, M. L. Verardi, D. R. Hyde, *Neuron* **5**, 889 (1990).
23. C. S. Zuker, *Current Opin. in Neurobiol.* **2**, 622 (1992).
24. D. R. Hyde, K. L. Mecklenburg, J. A. Pollock, T. S. Vihtelic, S. Benzer, *Proc. Natl. Acad. Sci. U.S.A.* **87**, 1008 (1990).
25. D. P. Smith, B.-H. Shieh, C. S. Zuker, *ibid.*, p. 1003.
26. H. LeVine *et al.*, *Mech. Dev.* **33**, 19 (1990).
27. T. Yamada *et al.*, *Science* **248**, 483 (1990).
28. D. Van Vactor, Jr., D. E. Krantz, R. Reinke, S. L. Zipursky, *Cell* **52**, 281 (1988).
29. Isogenic *brown*; *scarlet* (*bw*; *st*) males were treated with EMS and crossed to *arr2¹*. The resulting F1 males were backcrossed individually to *arr2¹* females. The *hairy⁺* (*h⁺*) progeny from this cross were subjected to antibody test for the loss of Arr2 antigen.
30. The mutant arrestin genes were isolated by polymerase chain reaction (PCR) amplification of genomic DNA from the mutant stocks, in two (*arr2*) or three (*arr1*) overlapping genomic fragments. Two independent PCR fragments for each region were sequenced to eliminate the possibility of errors during PCR amplification. Chromosomal DNA from *arr1¹* mutants was subjected to Southern blot analysis to locate the site of the insertion. For quantitation of protein levels, ten heads from dark-reared wild-type and mutant flies were sonicated and processed. The relative amount of arrestin polypeptide in each mutant was quantified on a Phosphorimager (Molecular Dynamics, Sunnyvale, CA). Values are averages of three independent experiments.
31. P. J. Dolph and C. S. Zuker, unpublished observations.
32. The time constant τ was calculated by fitting an exponential function of the form $A(t) = A_0 e^{-t/\tau}$ to the tail of the deactivation phase of the light response.
33. K. Palczewski, J. Buczylo, N. R. Imami, J. H. McDowell, *J. Biol. Chem.* **266**, 15334 (1991).
34. V. V. Gurevich and J. L. Benovic, *ibid.* **267**, 21919 (1992).
35. R. Ranganathan and C. S. Zuker, unpublished observations.
36. E. A. Richard and J. Lisman, *Nature* **356**, 336 (1992).
37. M. T. F. Fuortes and A. L. Hodgkin, *J. Physiol.* **172**, 239 (1964); D. A. Baylor and A. L. Hodgkin, *J. Physiol.* **242**, 729 (1974).
38. B. Minke, in *The Molecular Mechanisms of Phototransduction*, H. Steive, Ed. (Springer-Verlag, New York, 1986) pp. 241–286.
39. Experiments in Fig. 5 were performed under voltage-clamp conditions. Therefore, the term prolonged inward current is appropriate. However, we use the term PDA throughout the text for contextual and historical reasons.
40. H. Matsumoto and T. Yamada, *Biochem. and Biophys. Res. Commun.* **177**, 1306 (1991).
41. W. L. Pak, in *Neurogenetics, Genetic Approaches to the Nervous System*, X. O. Breakfield, Ed. (Elsevier, New York, 1979), pp. 67–99.
42. B.-H. Shieh, M. A. Stammes, S. Seavello, G. L. Harris, C. S. Zuker, *Nature* **338**, 67 (1989); S. Schneuwly *et al.*, *Proc. Natl. Acad. Sci. U.S.A.* **86**, 5390 (1989).
43. J. E. O'Tousa *et al.*, *Cell* **40**, 839 (1985); C. S. Zuker, A. F. Cowman, G. M. Rubin, *ibid.* p. 851.
44. R. S. Stephenson, J. O'Tousa, N. J. Scavarda, L. L. Randall, W. L. Pak, in *Biology of Photoreceptors*, D. Cosens and D. Vince-Price, Eds. (Cambridge Univ. Press, Cambridge, United Kingdom, 1983), pp. 477–501.
45. H. Matsumoto, K. Isono, Q. Pye, W. L. Pak, *Proc. Natl. Acad. Sci. U.S.A.* **84**, 985 (1987); C. Montell and G. Rubin, *Cell* **52**, 757 (1988).
46. B. Ondek *et al.*, *J. Biol. Chem.* **267**, 16460 (1992).
47. G. L. Fain and H. R. Matthews, *Trends Neurosci.* **13**, 378 (1990).
48. N. Colley and C. S. Zuker, unpublished observations.
49. B. Bloomquist *et al.*, *Cell* **54**, 723 (1988).
50. J. Pitcher, M. J. Lohse, J. Codina, M. G. Caron, R. J. Lefkowitz, *Biochemistry* **31**, 3193 (1992).
51. N. Colley, E. Baker, M. Stammes, C. Zuker, *Cell* **67**, 255 (1991).
52. T. Grigliatti, in *Drosophila: A Practical Approach*, D. B. Roberts, Ed. (IRL Press, Oxford, United Kingdom, 1986), pp. 39–58.
53. The *Df(2L)1131* was obtained from C. Goodman (University of California, Berkeley) and characterized by genetic complementation to linked markers, and mapped by in situ hybridizations to polytene chromosomes with an *arr1* probe. This deficiency completely deletes the *arr1* gene.
54. U. K. Laemmli, *Nature* **227**, 680 (1970).
55. D. P. Smith *et al.*, *Science* **254**, 1478 (1991).
56. R. Feiler *et al.*, *J. Neurosci.* **12**, 3862 (1992).
57. We thank D. Malicki for generating and purifying the antibodies to Arr1 and Arr2 used for immunocytochemistry; M. Whitney for help in constructing *arr1* and *arr2* transgenes; and A. E. Lougheed, M. J. Dolph, D. Malicki, D. M. Cowan, and C. Wilson for help in *Drosophila* stock maintenance and generating protein extracts for immunoblot analysis; D. Lindsley, C. Stevens, D. Baylor, and members of the Zuker Laboratory for helpful discussions. Supported by a program project grant from the NIH (C.S.Z.), by a National Eye Institute (NEI) postdoctoral fellowship (P.J.D.), by a training grant from the medical scientist training program (R.R.), and by a grant from NEI (N.J.C.).

1 March 1993; accepted 28 May 1993